https://doi.org/10.18321/cpc21(3)147-157

Magnetite nanoparticles obtained by solution combustion synthesis

B. Kaidar, A. Lesbayev, A. Imash*, D. Baskanbayeva, D. Akalim, A. Keneshbekova, E. Yensep, A. Ilyanov, G. Smagulova

Satbayev University, 22a Satbayev str., Almaty, Kazakhstan

ABSTRACT

This research presents a comprehensive investigation into the synthesis and characterization of magnetite nanoparticles through solution combustion reactions ignited by conventional means. In addition to the structural and compositional findings, this study's main investigation results include the specific surface area measurements conducted using the BET method. The analysis revealed specific surface area values for the synthesized magnetite nanoparticles at varying propellant-to-oxidant ratios, demonstrating a substantial decrease in specific surface area as the ratio increased. Specifically, specific surface areas of 72.203 m^2/g for the 1:1 ratio, 22.240 m^2/g for the 1:1.5 ratio, and 9.204 m^2/g for the 1:2 ratio were determined. Furthermore, calculations based on the BET results and assuming spherical magnetite nanoparticles provided average particle sizes of 16±1 nm for the 1:1 ratio, 51±2 nm for the 1:1.5 ratio, and 125±4 nm for the 1:2 ratio. These findings highlight the impact of synthesis parameters on the nanoparticles' surface area and size, shedding light on their potential applications in various fields, including nanomedicine and magnetic diagnostics. Overall, this research contributes valuable insights into the synthesis, characterization, and tunable properties of magnetite nanoparticles, offering potential avenues for their utilization across diverse industries.

Keywords: Solution combustion synthesis, magnetite nanoparticles, metal oxides

1. Introduction

Nanotechnology, situated at the convergence of science, engineering, and materials science, has ushered in revolutionary breakthroughs across various industrial sectors. Notably, the magnetic properties of materials find extensive utility in science and technology, contributing to advancements in acoustic systems [1], proximity sensors [2], electrical machinery [3], magnetic separators [4], as well as everyday consumer electronics like mobile phones and cameras [5]. The shift towards the nanoscale has catalyzed the emergence of a novel realm within magnetic materials science: magnetic nanomaterials. The composition, structure, and properties of magnetic nanomaterials exhibit wide-ranging diversity, contingent upon the starting materials, synthesis techniques, and the practical challenges they are designed to address. Predominantly, magnetic nanomaterials are derived from elements such as Ni, Co, and Fe [6]. Within this domain, Fe-based compounds, particularly Fe_3O_4 magnetite, assume a prominent role.

Magnetite nanoparticles, composed of iron oxide (Fe_3O_4) and characterized by their diminutive size on the nanoscale, showcase a plethora of intriguing properties that set them apart from their macroscopic counterparts. Notably, they play a pivotal role in the realm of nanomedicine, contributing to the development of innovative magnetic diagnostic methodologies such as magnetoresistance and microHall (μHall) biosensors [7, 8].

In line with the classification of nanomaterials based on their geometric and structural attributes, magnetic nanomaterials can assume zero-dimensional (0D) structures, represented by magnetic nanoparticles and nanopowders. Additionally, one-dimensional (1D) configurations encompass magnetic nanofibers, nanorods, nanotubes, and other elongated forms [9]. The synthesis of magnetite nanoparticles has garnered substantial interest among researchers due to their vast potential applications. The table below provides a concise summary of the primary methods employed for the synthesis of magnetite nanoparticles.

While magnetite nanoparticles hold immense potential across diverse industries, they are

*Ответственный автор
E-mail: iimash.aigerim@gmail.com

Table 1. Methods of production of magnetite nanoparticles.

№	Method	Advantages	Disadvantages	Ref.
1	Co-precipitation	Simple and economical	1. Wide size distribution 2. Risk of agglomeration	[10-12]
2	Solvothermal/ hydrothermal synthesis	Controlled particle growth	1. Requires specialised equipment 2. Long reaction time 3. Energy intensive process	[13]
3	Thermal decomposition	High monodispersity	1. Accurate control of temperature and reaction conditions 2. Energy intensive process 3. Potential risks with some starting materials	[14]
4	Microemulsions	Size control	1. Involves the use of surfactants, which may require additional cleaning steps 2. Difficult microemulsion conditions 3. Moderate yield	[15]
5	Sol-gel	High purity	1. Slow process 2. Requires specialised equipment 3. Effect of choice of starting materials	[16]

accompanied by a set of challenges that warrant careful consideration. The synthesis of uniform nanoparticles with precise control over size and shape remains a complex and cost-intensive endeavor. Researchers must navigate the delicate balance between achieving desired properties and ensuring scalability for industrial utilization.

Furthermore, the seamless integration of magnetite nanoparticles into various industries necessitates rigorous safety assessments, particularly in biomedical and environmental contexts. Prioritizing biocompatibility and conducting thorough toxicity evaluations are paramount, as any adverse effects could compromise the advantages of these nanoparticles [17].

In the realm of environmental applications, continued research is imperative to assess the cost-effectiveness and long-term sustainability of magnetite nanoparticle-based remediation systems. Factors such as maintenance, remediation efficiency, and recycling strategies must be taken into account to determine their practical viability.

Among the myriad methods available for nanoparticle production, the solution combustion method emerges as an appealing and efficient approach. This technique leverages the exothermic nature of chemical reactions to swiftly generate nanoparticles under controlled conditions, rendering it an attractive choice for producing magnetite nanoparticles with meticulous control over size, morphology, and magnetic properties [18].

Consequently, this study endeavors to expand the existing knowledge base on magnetite nanoparticles, elucidate the synthesis process of solution combustion, characterize the resulting nanoparticles comprehensively, and shed light on their potential applications.

2. Experimental part

2.1. Materials

The following materials and equipment were used for the synthesis of magnetite nanoparticles by solution combustion: ferric nitrate ($Fe(NO_3)_3 \cdot 9H_2O$); citric acid ($C_6H_8O_7 \cdot 6H_2O$) of analytical purity, without further purification; magnetic stirrer (ISOLAB); ultrasonic bath (Grad Technology).

2.2. Method for obtaining of magnetite (Fe_3O_4) nanoparticles

Magnetic Fe_3O_4 magnetite nanoparticles were prepared by solution combustion at different oxidant ratios. Iron nitrate ($Fe(NO_3)_3 \cdot 9H_2O$) and citric acid ($C_6H_8O_7 \cdot 6H_2O$) of analytical purity, without further purification, were used as starting components.

Varying the ratio of fuel to oxidant changes the pH of the initial solution and affects the dispersibility of the final product obtained. The synthesis of magnetite nanoparticles was carried out at the following iron nitrate to citric acid ratios: 1:1, 1:1.5 and 1:2.

The process of solution combustion occurs as a result of the chemical interaction between citric acid and iron nitrate according to the reaction below:

$$54Fe(NO_3)_3 \cdot 9H_2O + 46C_6H_8O_7 \cdot 6H_2O \rightarrow 18Fe_3O_4 + 276CO_2 + 716H_2O + 81N_2 \quad (1)$$

Magnetite nanoparticles were collected by magnetic field, washed several times with water, and then dried.

2.3 Methods of research of the obtained samples

2.3.1. X-ray phase analysis

The MiniFlex X-ray diffractometer, a cutting-edge 5th generation instrument, was employed for the comprehensive qualitative and quantitative analysis of polycrystalline materials. Operating under precise imaging settings, including adjustable X-ray tube voltage (up to 40 kV), a constant tube current (15 mA), goniometer step movements as fine as 0.02 degrees 2θ for spot intensity measurements, a consistent sample rotation speed of 10 rpm within its own plane, and a scanning range spanning from 3 to 90 degrees 2θ, this instrument ensured meticulous data collection. The use of a Kβ filter enabled monochromatization of X-ray radiation, enhancing measurement accuracy. Subsequent data processing and analysis were conducted with the PDXL database, offering advanced capabilities for interpreting the acquired data. This holistic approach facilitated a comprehensive and precise evaluation of the crystalline characteristics of the materials, affording valuable qualitative and quantitative insights into their composition and structure for diverse scientific and industrial applications.

2.3.2. Electron and optical microscopy

The investigation into the structure, dimensions, and morphology of the acquired samples was conducted utilizing a Quanta 200i 3D scanning electron microscope (FEI, USA) with an accelerating voltage of 30 kV. This microscopy analysis was performed at the "National Nanotechnology Laboratory of Open Type," (al-Farabi Kazakh National University, Almaty, Kazakhstan). The utilization of this method enabled the determination of surface structures in volumetric imagery, facilitating the evaluation of both structural features and the sizing of individual particles. It is worth noting that the Quanta 200i 3D SEM is equipped with an energy dispersive X-ray system (EDS), allowing for the analysis of a wide range of chemical elements spanning from B to U. The energy resolution of this system is 132 eV (Mn Kα). EDS analysis was employed to ascertain the elemental composition of magnetite nanoparticles.

For the examination of microcracks in fibers and the determination of mesophase centers in carbon pitches, a LeciaDM 600 M automated digital optical microscope, located at the "National Nanotechnology Laboratory of Open Type," (al-Farabi Kazakh National University, Almaty, Kazakhstan), was employed. This optical microscope facilitates work with magnifications ranging from 150x to 1500x.

2.3.3. Measurement of specific surface area

The specific surface area of the samples was determined utilizing the BET (Brunauer-Emmett-Teller) method through thermal desorption of inert gases, employing the SORBTOMETR-M instrument. This selection of methodology was driven by several advantageous features compared to static techniques. Notably, it obviates the need for a vacuum apparatus, offers straightforward installation, and facilitates automation. The core principle involves the dynamic desorption of gas-adsorbate from the surfaces of the test materials. In the BET method, a helium-nitrogen mixture with predefined composition is directed through an adsorber housing the sample. Following degassing, achieved by elevating the sample's temperature within a stationary gas stream at a specified level, previously adsorbed gases are desorbed from the sample surface. Furthermore, specific surface area measurements were conducted employing helium gas as the carrier, blended with argon at a flow rate of 48–50 ml/min, and the argon concentration in the mixture ranged from 3% to 6%. The sample suspension quantity ranged from 0.03 to 0.15 g. The associated measurement error was limited to 5% [19].

2.3.4. Measurement of magnetic properties of samples

Magnetic moment values of the studied material samples were assessed using a 14T Cryogenic vibrating sample magnetometer (VSM), which comprises the following components: 1) a mechanical vibration generator; 2) a rod affixed with a quartz sample holder containing the material under examination; 3) an electronic measurement unit. Before conducting measurements, the sample of the material being investigated was enclosed within a plastic tube and securely fastened between the clamps of the rod. Mechanical vibrations were generated using an electrodynamic loudspeaker, with a rod serving to transmit these vibrations from the generator to the sample. The vibration amplitude of the sample was maintained at 0.03 meters, with a frequency of 200 Hz. A capacitive sensor was employed to stabilize the vibration amplitude. Following phase detection and amplification, the signal from the measuring coils

was directed to the input of the Hall sensor. The data from the measurement of signal parameters, including the magnetic moment of the investigated material sample and the magnetic field induction within it, were documented using a personal computer [20-22].

3. Results and discussion

This research is centered on the synthesis of magnetic iron oxides through solution synthesis combustion reactions initiated by conventional ignition. Initially, a thorough examination of the characteristics of iron oxide nanoparticles generated through conventional ignition combustion reactions was conducted.

In our study, we conducted a comprehensive investigation of magnetite nanoparticles using advanced techniques such as XRF, optical microscopy and SEM with EDS-analysis.

To ascertain the crystal structure of the magnetite nanoparticles synthesized through solution combustion, we conducted X-ray diffraction analysis using a MiniFlex 300/600 diffractometer, as illustrated in Fig. 1 (g-k). This analysis aimed to explore the impact of varying the concentration ratio between the propellant (citric acid) and the oxidant (ferric nitrate) on both the crystal structure and the crystallite sizes of the nanoparticles.

Crystallite sizes were determined using the Williamson-Hall method with the instrument's standard software. For the 1:1 ratio, the crystallite size was calculated to be 178 angstroms (Å), while for the 1:1.5 ratio, it was found to be 100 Å, and for the 1:2 ratio, the crystallite size measured 143 Å.

Based on the outcomes of X-ray diffraction analysis carried out utilizing the MiniFlex 300/600 diffractometer, the crystalline phase identified within the samples was confirmed to be magnetite (Fe_3O_4). Notably, variations in the concentration ratio of the fuel to oxidant were observed to exert a direct influence on the size of the crystallites.

Alterations in the ratio of the initial constituents, namely iron nitrate and citric acid, as well as adjustments in the synthesis parameters, result in noteworthy modifications in the structure and composition of the ultimate product. Comprehensive elemental analysis (Fig. 1d-f) was conducted on the iron oxide samples across all three ratios (1:1, 1:1.5, 1:2). The investigations revealed a notable trend wherein the percentage of carbon content in the final product exhibited an increase proportionate to the higher concentration of the oxidant, indicating a direct correlation between oxidant concentration and carbon content in the synthesized materials.

Figure 1a-c depict optical images of magnetite nanoparticles obtained under varying ratios of fuel to oxidant concentration. Optical microscopy investigations of these magnetite nanoparticle samples have revealed the presence of carbon. These studies have unveiled a significant phenomenon in the synthesis process by the solution combustion method, where magnetite nanoparticles undergo sintering with concurrently formed carbon. The resultant material exhibits a profusion of macropores and channels, a consequence of the release of substantial quantities of gaseous products stemming from the reaction between iron nitrate and citric acid.

To delve deeper into the morphology and structure of the magnetite nanoparticles synthesized through the solution combustion method, scanning electron microscopy was employed. SEM images of the acquired samples are depicted in Fig. 1d-f. These examinations have elucidated that during the synthesis process, magnetite nanoparticles agglomerate and coalesce into conglomerates characterized by a layered structure. Particularly noteworthy is the prevalence of the amorphous phase, especially within agglomerates surpassing the 100 nm scale. To ensure uniform dispersion of magnetite nanoparticles in the shielding material, separation of these agglomerates was carried out through ultrasonic pretreatment of nanomagnetite nanoparticle powders in aqueous suspension.

Furthermore, the outcomes of the EDS analysis have unveiled a correlation between the fuel-to-oxidant concentration ratio in the solution combustion reaction and the resultant composition and structure of the samples. An increase in fuel concentration is associated with an augmented predominance of amorphous carbon in the samples, as evidenced by carbon content percentages of 24.37% at the stoichiometric ratio (1:1), 32.7% at the 1:1.5 ratio, and 38.06% at the 1:2 ratio.

The specific surface area of all synthesized samples of magnetite nanoparticle powders was determined using the BET-analysis. The specific surface area analysis results for magnetite nanoparticles, along with calculations of the average size of the products obtained at varying stoichiometric ratios of propellant to oxidant, are presented in Table 2 below. The BET method revealed specific surface area values of 72.203 m^2/g for the 1:1 ratio, 22.240 m^2/g for the 1:1.5 ratio, and 9.204 m^2/g for the 1:2 ratio.

The structural characteristics of the synthesized nanoparticles were found to be significantly influenced by the ratio of propellant to oxidant.

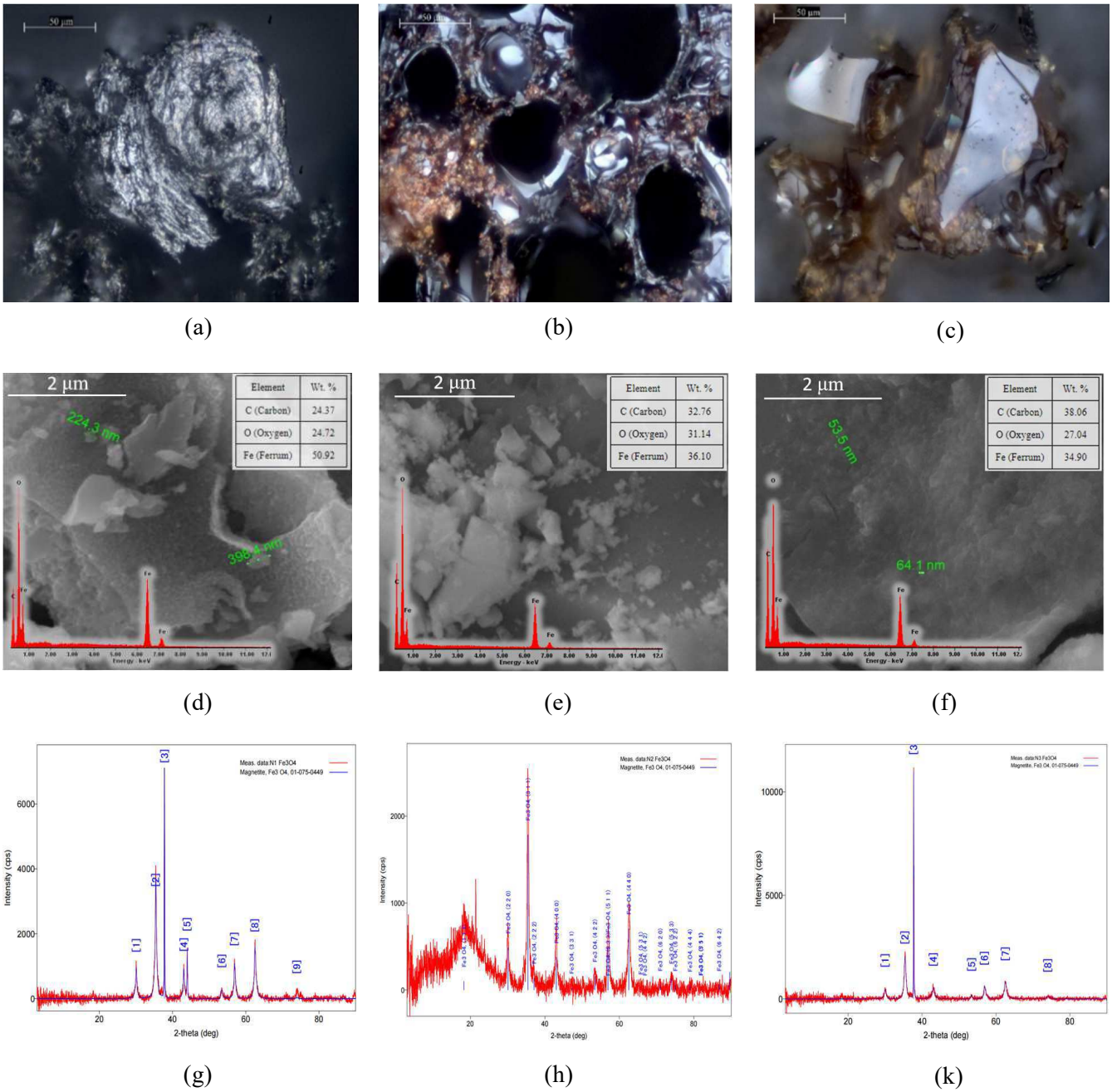

Fig. 1. Optical, SEM images with EDS spectrum and XRF patterns of obtained magnetite nanoparticles for the iron nitrate to citric acid ratios: 1:1 (a,d,g), 1:1.5 (b,e,h) and 1:2 (c,f,k).

Specifically, three distinct ratios of iron nitrate to citric acid (1:1, 1:1.5, 1:2) were systematically investigated. X-ray phase analysis underscored the pivotal role played by the initial component ratio in the synthesis of magnetite (Fe_3O_4) nanoparticles. A comprehensive evaluation of the structure and morphology was undertaken through optical and scanning electron microscopy (SEM). The optical microscopy results unveiled the presence of carbon in the synthesized magnetite nanoparticle samples, with the synthesis process involving sintering of magnetite nanoparticles alongside the formation of carbon. SEM studies corroborated this observation by revealing the agglomeration of magnetite nanoparticles into conglomerates characterized by a layered structure. Moreover, the predominant presence of an amorphous phase, particularly evident in clusters exceeding 100 nm in size, was noted.

Additionally, the specific surface area analysis conducted using the BET method elucidated specific surface area values of 72.203 m^2/g for the 1:1 ratio, 22.240 m^2/g for the 1:1.5 ratio, and 9.204 m^2/g for the 1:2 ratio. Based on the obtained data, calculations were performed to deduce the average sizes of magnetite nanoparticles synthesized via the solution combustion method. These calculations, under the

Table 2. Particle size as a function of fuel/oxidiser ratio

Stoichiometric ratio	Phase name (XRF)	LXRF, nm	S_{BET} (m^2/g)	D_{BET}, nm	Carbon content, %
$Fe(NO_3):C_6H_8O_7$, 1:1	Fe_3O_4-magnetite	20	72.203	16±1	24.37
$Fe(NO_3):C_6H_8O_7$, 1:1,5	Fe_3O_4-magnetite	18	22.240	51±2	32.7
$Fe(NO_3):C_6H_8O_7$, 1:2	Fe_3O_4-magnetite	13	9.204	125±4	38.06

assumption of spherical magnetite nanoparticles, yielded an average particle size of 16±1 nm for the 1:1 ratio, 51±2 nm for the 1:1.5 ratio, and 125±4 nm for the 1:2 ratio.

The magnetic properties of nanoparticles are intricately influenced by a multitude of factors, including their chemical composition, crystal lattice type, structural defects, particle size, shape, and morphology. Consequently, through careful material selection and the manipulation of synthesis conditions, it is possible to finely tune the magnetic properties of the resulting nanomaterials, albeit within certain constraints. The ferromagnetic attributes of materials exhibit a strong size dependency, with individual particles encountering thermal fluctuations as they diminish in size, ultimately leading to a nullification of the collective magnetization of the particle ensemble. However, when nano-sized particles are exposed to a sufficiently robust magnetic field, their potential energy of magnetization surpasses the energy associated with thermal fluctuations. This phenomenon causes them to behave as ferromagnets while in the magnetic field, giving rise to their superparamagnetic properties.

The magnetic moment values of the magnetite nanoparticles obtained in this study were assessed using a Cryogenic 14T vibrating sample magnetometer. The results of these measurements for a 1:1 sample are graphically presented in Fig. 2a, 2b. The conducted investigations have revealed that the magnetite nanoparticles transition to a superparamagnetic state, as evidenced by the absence of hysteresis in the field magnetization curve. This transition to the superparamagnetic state can be attributed to the nanoparticles' transition into a single-domain state, where uniform magnetization prevails throughout the volume.

4. Outlook

Nanosized magnetite nanoparticles and composites based on them are a potential material for the future with a wide range of applications. This material is also unique due to its high electromagnetic characteristics. Table 3 shows the main parameters and possibilities for using magnetite nanoparticles.

Thus, according to the table, it can be seen that magnetite nanoparticles obtained by the solution combustion method can play an important role in the production and use of composite materials. This once again proves a number of advantages of the method of obtaining magnetic nanoparticles and their future application.

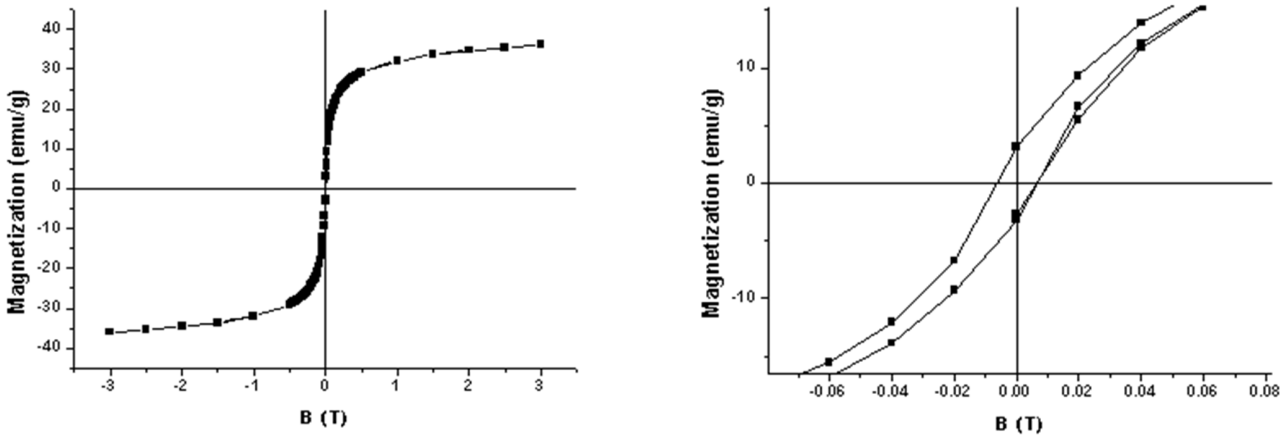

(a) (b)

Fig. 2. Magnetic hysteresis of magnetite nanoparticles (ratio 1:1) at room temperature.

Table 3. Summary of applications of composite material based on magnetite nanoparticles

Composite material based on iron oxide	Synthesis method of Fe_3O_4	Particle size	BET[$m^2 \cdot g^{-1}$]	Application	Ref.
Fe_3O_4	Microwave combustion	20–25 nm	72.53	Possible in all	[23]
Fe_3O_4	Solution combustion	250–350 nm	83.4		[24]
Fe_3O_4	Solution combustion	19.9–48 nm	N/A		[25]
Fe_3O_4/Fe_2O_3	Solution combustion	67nm	20.85	Medicine	[26]
Fe_3O_4/FeO_3/*rGO	Sol-gel auto-combustion	37 ± 2 nm	13.3959	Pharmacology	[27]
Fe_3O_4/CuO	Combustion	32 nm	N/A	Agriculture	[28]
Fe_2O_3/Fe_3O_4	Rapid combustion	42 nm	N/A	Biotechnology	[29]
Fe_3O_4/C	Combustion	<10 mm	21.9	Energy (lithium-ion batteries)	[30]
Fe_3O_4/C	Solution combustion	100 nm	N/A	Electric shielding	[31]
Fe_3O_4/Ag/C	Combustion	10 ± 2 nm	744.7	Environmental(dyes removal)	[32]

*rGO - Reduced graphene oxide

5. Conclusion

In this study, we explored the synthesis and characterization of magnetite nanoparticles through solution synthesis combustion reactions initiated by conventional ignition. Our investigation encompassed a thorough analysis of these nanoparticles, employing advanced techniques such as XRF, optical microscopy, SEM with EDS-analysis, and X-ray diffraction. Notably, our findings elucidated the crucial role played by the propellant-to-oxidant concentration ratio in influencing the crystal structure and crystallite size of the synthesized magnetite nanoparticles. Elemental analysis revealed a direct correlation between oxidant concentration and carbon content in the final product. Optical microscopy and SEM investigations unveiled the presence of carbon and the sintering phenomenon, leading to the formation of macropores and channels. Additionally, BET analysis provided specific surface area values that varied with the concentration ratio. Magnetic property assessments demonstrated the transition of magnetite nanoparticles to a superparamagnetic state, indicative of their potential utility in diverse applications. This comprehensive exploration contributes to the understanding of magnetite nanoparticles and their prospects across various fields, offering valuable insights for future nanomaterial research and development.

Acknowledgments

This work was supported by the Ministry of Science and Higher Education of the Republic of Kazakhstan (Grant No AP19679690).

References

[1]. Liang B., Li Z., Dixon S., Yu Y., Zhai G. Development of a magnetostrictive Fe_3O_4-film electromagnetic acoustic transducer // Sensors and Actuators A: Physical. – 2023. – Vol. 361. – P. 114593.

[2]. Zhang W., Guo Q., Duan Y., Xing C., Peng Z. A textile proximity/pressure dual-mode sensor based on magneto-straining and piezoresistive effects // IEEE Sensors Journal. – 2022. – Vol. 22. – No. 11. – P. 10420-10427.

[3]. Zeng Z., Zhao H., Wang J., Lv P., Zhang T., Xia Q. Nanostructured Fe_3O_4@ C as anode material for lithium-ion batteries // Journal of Power Sources. – 2014. – Vol. 248. – P. 15-21.

[4]. Yavuz C.T., Mayo J.T., Yu W.W., Prakash A., Falkner J.C., Yean S., Cong L., Shipley H.J., Kan A., Tomson M., Natelson D., Colvin V.L. Low-field magnetic separation of monodisperse Fe3O4 nanocrystals // Science. – 2006. – Vol. 314. – No. 5801. – P. 964-967.

[5]. Chakraborty I., Bose S., Chatterjee K. Designer Fe_3O_4@ Ag Core–Shell Porous Nanospheres for Enhanced Electromagnetic Interference Shielding of Polymer Nanocomposites // Advanced Engineering Materials. – 2023. – P. 2201363.

[6]. Chavan N., Dharmaraj D., Sarap S., Surve C. Magnetic nanoparticles – A new era in nanotechnology // Journal of Drug Delivery Science and Technology. – 2022. – P. 103899.

[7]. Huang H.T., Garu P., Li C.H., Chang W.C., Chen B.W., Sung S.Y., Lee C.M., Chen J.Y.,

Hsieh T.F., Sheu W.J., Ouyang H., Wang W.C., Chang C.R., Wang C.L., Hsu M.S., Wei Z.H. Magnetoresistive biosensors for direct detection of magnetic nanoparticle conjugated biomarkers on a chip // Spin – World Scientific Publishing Company, 2019. – Vol. 9. – No. 02. – P. 1940002.

[8]. Kazakova O., Gallop J., Perkins G., Cohen L. Scanned micro-Hall microscope for detection of biofunctionalized magnetic beads // Applied physics letters. – 2007. – Vol. 90. – No. 16.

[9]. Nguyen M.D., Tran H.V., Xu S., Lee T.R. Fe_3O_4 Nanoparticles: Structures, synthesis, magnetic properties, surface functionalization, and emerging applications // Applied Sciences. – 2021. – Vol. 11. – No. 23. – P. 11301.

[10]. Lin C.C., Lai Y.P., Wu K.Y. A high-productivity process for mass-producing Fe_3O_4 nanoparticles by co-precipitation in a rotating packed bed // Powder Technology. – 2022. – Vol. 395. – P. 369-376.

[11]. Mansurov Z.A., Smagulova G.T., Kaidar B.B., Lesbaev A.B., Imash A. Preparation of fibers based on polyacrylonitrile with the addition of magnetite nanoparticles // News of universities. Powder metallurgy and functional coatings. – 2021. – Vol. 4. – P. 68-76.

[12]. Mansurov Z., Smagulova G., Kaidar B., Imash A., Lesbayev A. PAN–Composite Electrospun-Fibers Decorated with Magnetite Nanoparticles // Magnetochemistry. – 2022. – Vol. 8. – №. 11. – P. 160.

[13]. Su M., He C., Shih K. Facile synthesis of morphology and size-controlled α-Fe_2O_3 and Fe_3O_4 nano-and microstructures by hydrothermal/ solvothermal process: the roles of reaction medium and urea dose // Ceramics International. – 2016. – Vol. 42. – No. 13. – P. 14793-14804.

[14]. Vuong T.K.O., Lai Y.P., Wu K.Y. Synthesis of high-magnetization and monodisperse Fe_3O_4 nanoparticles via thermal decomposition // Materials Chemistry and Physics. – 2015. – Vol. 163. – P. 537-544.

[15]. Lu T., Wang J., Yin J., Wang A., Wang X., Zhang T. Surfactant effects on the microstructures of Fe_3O_4 nanoparticles synthesized by microemulsion method // Colloids and Surfaces A: Physicochemical and Engineering Aspects. – 2013. – Vol. 436. – P. 675-683.

[16]. Lemine O.M., Omri K., Zhang B., El Mir L., Sajieddine M., Alyamani A., Bououdina M. Sol–gel synthesis of 8 nm magnetite (Fe_3O_4) nanoparticles and their magnetic properties // Superlattices and Microstructures. – 2012. – Vol. 52. – No. 4. – P. 793-799.

[17]. Yew Y.P., Shameli K., Miyake M., Khairudin N.B. B.A., Mohamad S.E.B., Naiki T., Lee K.X. Green biosynthesis of superparamagnetic magnetite Fe_3O_4 nanoparticles and biomedical applications in targeted anticancer drug delivery system: A review // Arabian Journal of Chemistry. – 2020. – Vol. 13. – No. 1. – P. 2287-2308.

[18]. Parnianfar H., Masoudpanah S.M., Alamolhoda S., Fathi H. Mixture of fuels for solution combustion synthesis of porous Fe_3O_4 powders // Journal of Magnetism and Magnetic Materials. – 2017. – Vol. 432. – P. 24-29.

[19]. Vyacheslavov A.S., Pomerantseva E.A. Measurement of surface area and porosity by capillary condensation of nitrogen: methodical development. – M., 2006. – P. 55.

[20]. Rezinkina, M.M. Numerical Calculation of the Magnetic Field and Magnetic Moment of Ferromagnetic Bodies of Complex Spatial Configuration / M.M. Rezinkina // Journal of Technical Physics. – 2009. – Vol. 79, Issue 8. – P. 8-17.

[21]. Velikanov D.A., Yurkin G.Y., Patrin G.S. Stabilization of Sample Mechanical Oscillation Parameters in a Vibrating Magnetometer // Nauchnoe priborostroenie. – 2008. – No 3. – P. 86-94.

[22]. Neamakh M.R., Sokolov V.B. Magnetic Properties of Furnace Gas Cleaning Sludge // Doklady BSUIR. – 2013. – No 2 (72). – P. 26-30.

[23]. Manikandan A., Vijaya J.J., Mary J.A., Kennedy L.J., Dinesh A. Structural, optical and magnetic properties of Fe_3O_4 nanoparticles prepared by a facile microwave combustion method //Journal of Industrial and Engineering Chemistry. – 2014. – Vol. 20. – №. 4. – P. 2077-2085.

[24]. Parnianfar H., Masoudpanah S.M., Alamolhoda S., Fathi H. Mixture of fuels for solution combustion synthesis of porous Fe_3O_4 powders //Journal of Magnetism and Magnetic Materials. – 2017. – Vol. 432. – P. 24-29.

[25]. Wang X., Qin M., Cao Z., Jia B., Gu Y., Qu X., Volinsky A.A. Growth mechanism and magnetism in carbothermal synthesized Fe_3O_4 nanoparticles from solution combustion precursors //Journal of Magnetism and Magnetic Materials. – 2016. – Vol. 420. – P. 225-231.

[26]. Liu R., Huang W., Pan S., Li Y., Yu L., He D. Covalent immobilization and characterization of penicillin G acylase on magnetic Fe_2O_3/ Fe_3O_4heterostructure nanoparticles prepared via a novel solution combustion and gel calcination process // International Journal of Biological Macromolecules. – 2020. – Vol. 162. – P. 1587-1596.

[27]. Baladi M., Amiri M., Salavati-Niasari M. Green sol–gel auto-combustion synthesis, characterization and study of cytotoxicity and anticancer activity of $ErFeO_3$/Fe_3O_4/rGO nanocomposite // Arabian Journal of Chemistry. – 2023. – Vol. 16. – №. 4. – P. 104575.

[28]. Yeganeh-Faal A., Kadkhodaei M. A new combustion method for the synthesis of copper oxide nano sheet and Fe_3O_4/CuO magnetic

nanocomposite and its application in removal of diazinon pesticide // Results in Engineering. – 2022. – Vol. 16. – P. 100599.

[29]. Huang W., Pan S., Li Y., Yu L., Liu R. Immobilization and characterization of cellulase on hydroxy and aldehyde functionalized magnetic Fe_2O_3/Fe_3O_4 nanocomposites prepared via a novel rapid combustion process // International Journal of Biological Macromolecules. – 2020. – Vol. 162. – P. 845-852.

[30]. Han C.G., Sheng N., Zhu C., Akiyama T. Cotton-assisted combustion synthesis of Fe_3O_4/C composites as excellent anode materials for lithium-ion batteries // Materials Today Energy. – 2017. – Vol. 5. – P. 187-195.

[31]. Meng X., Yang W., Han G., Yu Y., Ma S., Liu W., Zhang Z. Three-dimensional foam-like Fe_3O_4@C core-shell nanocomposites: controllable synthesis and wideband electromagnetic wave absorption properties // Journal of Magnetism and Magnetic Materials. – 2020. – Vol. 502. – P. 166518.

[32]. Muntean S.G., Nistor M.A., Ianoș R., Păcurariu C., Căpraru A., Surdu V. A. Combustion synthesis of Fe_3O_4/Ag/C nanocomposite and application for dyes removal from multicomponent systems // Applied Surface Science. – 2019. – Vol. 481. – P. 825-837.

References

[1]. Liang B, Li Z, Dixon S, Yu Y, Zhai G (2023) Sensors and Actuators A: Physical 361:114593. https://doi.org/10.1016/j.sna.2023.114593

[2]. Zhang W, Guo Q, Duan Y, Xing C, Peng, Z (2022) IEEE Sensors Journal 22(11):10420-10427. https://doi.org/10.1109/JSEN.2022.3168068

[3]. Zeng Z, Zhao H, Wang J, Lv P, Zhang T, Xia Q (2014) Journal of Power Sources 248:15-21. https://doi.org/10.1016/j.jpowsour.2013.09.063

[4]. Yavuz CT, Mayo JT, Yu WW, Prakash A, Falkner JC, Yean S, Colvin VL (2006) Science 314(5801):964-967. https://doi.org/10.1126/science.1131475

[5]. Chakraborty I, Bose S, Chatterjee K (2023 Advanced Engineering Materials 25:2201363. https://doi.org/10.1002/adem.202201363

[6]. Chavan N, Dharmaraj D, Sarap S, Surve C (2022) Journal of Drug Delivery Science and Technology 77:103899. https://doi.org/10.1016/j.jddst.2022.103899

[7]. Huang HT, Garu P, Li CH, Chang WC, Chen BW, Sung SY, Wei ZH (2019, June) In Spin. World Scientific Publishing Company 9(2):1940002. https://doi.org/10.1142/S2010324719400022

[8]. Kazakova O, Gallop J, Perkins G, Cohen L (2007) Applied physics letters 90(16). https://doi.org/10.1063/1.2724770

[9]. Nguyen MD, Tran HV. Xu S, Lee TR. (2021) Applied Sciences 11(23):11301. https://doi.org/10.3390/app112311301

[10]. Lin CC, Lai YP, Wu KY (2022) Powder Technology 395:369-376. https://doi.org/10.1016/j.powtec.2021.09.036

[11]. Mansurov ZA, Smagulova GT, Kaidar BB, Lesbaev AB, Imash A. (2021) Powder Metallurgy and Functional Coatings (4):68-76. https://doi.org/10.17073/1997-308X-2021-4-68-76

[12]. Mansurov Z, Smagulova G, Kaidar B, Imash A, Lesbayev A (2022) Magnetochemistry 8(11):160. https://doi.org/10.3390/magnetochemistry8110160

[13]. Su M, He C, Shih K (2016) Ceramics International 42(13):14793-14804. https://doi.org/10.1016/j.ceramint.2016.06.111

[14]. Vuong TKO, Le TL, Pham DV, Pham HN, Le Ngo TH, Do HM, Nguyen XP (2015) Materials Chemistry and Physics 163:537-544. https://doi.org/10.1016/j.matchemphys.2015.08.010

[15]. Lu T, Wang J, Yin J, Wang A, Wang X, Zhang T (2013) Colloids and Surfaces A: Physicochemical and Engineering Aspects 436:675-683. https://doi.org/10.1016/j.ceramint.2016.06.111

[16]. Lemine OM, Omri K, Zhang B, El Mir L, Sajieddine M, Alyamani A, Bououdina M (2012 Superlattices and Microstructures 52(4):793-799. https://doi.org/10.1016/j.spmi.2012.07.009

[17]. Yew YP, Shameli K, Miyake M, Khairudin N BBA, Mohamad, SEB, Naiki T, Lee K.X (2020) Arabian Journal of Chemistry 13(1):2287-2308. https://doi.org/10.1016/j.arabjc.2018.04.013

[18]. Parnianfar H, Masoudpanah SM, Alamolhoda S, Fathi H (2017) Journal of Magnetism and Magnetic Materials 432:24-29. https://doi.org/10.1016/j.jmmm.2017.01.084

[19]. Vyacheslavov AS, Pomerantseva EA, Gudilin EA (2006). Measurement of surface area and porosity by capillary condensation of nitrogen. The guidance paper, Moscow, Lomonosov Moscow State University. 30.

[20]. Rezinkina MM (2009) Technical Physics 54(8):1092-1101. https://doi.org/10.1134/S1063784209080027

[21]. Velikanov DA, Yurkin GY, Patrin GS (2008) Nauchnoe priborostroen (3):86-94.

[22]. Neamakh MR, Sokolov VB (2013) Doklady BSUIR 2(72):26-30.

[23]. Manikandan A, Vijaya JJ, Mary JA, Kennedy LJ, Dinesh A (2014) Journal of Industrial and Engineering Chemistry 20(4):2077-2085. https://doi.org/10.1016/j.jiec.2013.09.035

[24]. Parnianfar H, Masoudpanah SM, Alamolhoda S, Fathi H (2017) Journal of Magnetism and Magnetic Materials 432:24-29. https://doi.org/10.1016/j.jmmm.2017.01.084

[25]. Wang X, Qin M, Cao Z, Jia B, Gu Y, Qu X, Volinsky AA (2016) Journal of Magnetism and Magnetic Materials 420:225-231. https://doi.org/10.1016/j.jmmm.2016.07.030

[26]. Liu R, Huang W, Pan S, Li Y, Yu L, He D

(2020) International Journal of Biological Macromolecules 162:1587-1596. https://doi.org/10.1016/j.ijbiomac.2020.07.283
[27]. Baladi M, Amiri M, Salavati-Niasari M (2023) Arabian Journal of Chemistry 16(4):104575. https://doi.org/10.1016/j.arabjc.2023.104575
[28]. Yeganeh-Faal A, Kadkhodaei M (2022) Results in Engineering 16:100599. https://doi.org/10.1016/j.rineng.2022.100599
[29]. Huang W, Pan S, Li Y, Yu L, Liu R (2020) International Journal of Biological Macromolecules 162:845-852. https://doi.org/10.1016/j.ijbiomac.2020.06.209
[30]. Han CG, Sheng N, Zhu C, Akiyama T (2017) Materials Today Energy 5:187-195. https://doi.org/10.1016/j.mtener.2017.07.001
[31]. Meng X, Yang W, Han G, Yu Y, Ma S, Liu W, Zhang Z (2020) Journal of Magnetism and Magnetic Materials 502: 166518. https://doi.org/10.1016/j.jmmm.2020.166518
[32]. Muntean SG, Nistor MA, Ianoș R, Păcurariu C, Căpraru A, Surdu VA (2019) Applied Surface Science 481:825-837. https://doi.org/10.1016/j.apsusc.2019.03.161

Наночастицы магнитита полученные методом жидкофазного горения

Б. Кайдар, А. Лесбаев, А. Имаш*, Д. Басканбаева, Д. Акалим, А. Кенешбекова, Э. Енсеп, А. Ильянов, Г. Смагулова

Satbayev University, ул. Сатпаева 22а, Алматы, Казахстан

АННОТАЦИЯ

Данное исследование представляет собой комплексное исследование синтеза и характеристики наночастиц магнетита посредством реакций жидкофазного горения, зажигаемых обычными способами. Помимо структурных и композиционных данных, основные результаты исследования включают измерения удельной площади поверхности, проведенные с использованием метода БЭТ. Анализ выявил значения удельной поверхности синтезированных наночастиц магнетита при различных соотношениях пропеллента и окислителя, демонстрируя существенное уменьшение удельной поверхности по мере увеличения этого соотношения. В частности, были определены удельная площадь поверхности 72,203 м^2/г для соотношения 1:1, 22,240 м^2/г для соотношения 1:1,5 и 9,204 м^2/г для соотношения 1:2. Кроме того, расчеты, основанные на результатах БЭТ и предполагающие сферические наночастицы магнетита, дали средние размеры частиц 16±1 нм при соотношении 1:1, 51±2 нм при соотношении 1:1,5 и 125±4 нм при соотношении 1:2. Эти результаты подчеркивают влияние параметров синтеза на площадь и размер поверхности наночастиц, проливая свет на их потенциальное применение в различных областях, включая наномедицину и магнитную диагностику. В целом, это исследование вносит ценный вклад в синтез, характеристику и настраиваемые свойства наночастиц магнетита, предлагая потенциальные возможности для их использования в различных отраслях промышленности.

Ключевые слова: метод жидкофазного горения, наночастицы магнетита, оксиды металлов

Сұйық-фазалық жану синтезі арқылы алынған магнититті нанобөлшектер

Б. Кайдар, А. Лесбаев, А. Имаш*, Д. Басканбаева, Д. Акалим, А. Кенешбекова, Э. Енсеп, А. Ильянов, Г. Смагулова

Сәтбаев университеті, Сатпаев көшесі 22а, Алматы, Қазақстан

АННОТАЦИЯ

Бұл жұмыс магнетит нанобөлшектерінің синтезі мен сипаттамаларын қарапайым әдістермен тұтанатын сұйық фазалы жану реакциялары арқылы кешенді зерттеу болып табылады. Құрылымдық және композициялық деректерден басқа, зерттеудің негізгі нәтижелеріне БЭТ әдісімен жүргізілген бетінің нақты ауданын өлшеу кіреді. Талдау синтезделген магнетит нанобөлшектерінің меншікті бетінің мәндерін әр түрлі отын мен тотықтырғыш қатынасында анықтады, бұл арақатынас жоғарылаған сайын меншікті беттің айтарлықтай төмендеуін көрсетті. Нақтырақ, 1:1 қатынасы үшін 72,203 м^2/г, 1:1,5 қатынасы үшін 22,240 м^2/г және 1:2 қатынасы үшін 9,204 м^2/г бетінің меншікті ауданы анықталды. Сонымен қатар, БЭТ нәтижелеріне негізделген және сфералық магнетит нанобөлшектерін болжайтын есептеулер 1:1 қатынасында 16±1 нм, 1:1,5 қатынасында 51±2 нм және 1:2 қатынасында 125±4 нм бөлшектердің орташа өлшемдерін

берді. Бұл нәтижелер нанобөлшектердің ауданы мен бетінің өлшеміне синтез параметрлерінің әсерін көрсетеді, олардың наномедицина мен магниттік диагностиканы қоса алғанда, әртүрлі салаларда қолданылуын іске асырады. Тұтастай алғанда, бұл зерттеу магнетитті нанобөлшектердің синтезіне, сипаттамасына және реттелетін қасиеттеріне құнды үлес қосып, оларды әртүрлі өнеркәсіптік қолданбаларда пайдалану үшін әлеуетті қосымшаларды ұсынады.

Түйін сөздер: сұйық фазалық жану әдісі, магнетит нанобөлшектері, металл оксидтері